Journal of Applied Mechanics and Technical Physics, Vol. 35, No. 5, 1994

BUCKLING OF A BAR ON AN ELASTIC BASE

N. S. Astapov, A. G. Demeshkin, and V. M. Kornev

UDC 539.3

It is noted in [1] that a characteristic feature of the behavior of many structures under the action of compressive loads is periodicity of the initial buckling mode in the direction of compression upon loss of stability. However, the final buckling mode of such structures often has the form of a clearly defined single buckle or a small number of buckles. Buckling localization is due to the existence of a bifurcation point when the load reaches the maximal value or thereafter, at which the initial buckling mode bifurcates [1]; after bifurcation the periodic buckling mode is replaced by localized buckling, and this often takes place instantaneously. It is noted in [2] that the mechanism of buckling localization may consist of nonlinear interaction of the buckling modes with similar wavelengths. Study of the localization of buckling of models of real structures shows that the basic laws governing the process are described by the one-dimensional model of the behavior of a bar [1]. It is noted in [3] that the mechanism of buckling in a composite structure, in spite of specific peculiarities, is analogous to the mechanism of the buckling of a bar in an elastic medium.

In the present work we study experimentally the buckling of a flexible bar resting on an elastic base. We should point out the difficulties that arise in this problem. Thus, the validity of the Euler formula for the critical load of an axially compressed bar (1744) was finally confirmed 150 years later by the experiments of Bauschinger (1889), Considerć (1889), Tetmaier (1903), and von Karman (1910), in which much attention was devoted to the hinged support, central application of the compressive load, and the satisfaction of other conditions that are anticipated by the theory. Thanks to the adoption of these precautions, the experimental results approached the Euler load with accuracy to 1.5% [4]. The theoretical study of the problem of the buckling of bars resting on several elastic supports was first (1902) performed by Yasinskii [4, 5]. However, in spite of the fact that the theory of beams and plates resting on an elastic base is at the present time a very highly developed branch of mechanics, the existing computational methods are still far from perfect and do not answer many of the questions advanced by practical experience. It is noted in [6] that many of these methods are too complex for practical calculations; the hypotheses which are taken as the basis for the formulation of the mathematical models also can not be considered to be without fault.

In the present work we establish experimentally the possibility of unstable behavior of a bar resting on an elastic base, which agrees with the theoretical arguments. In the case of repeated loadings there is noted a reconfiguring of the buckling modes, which is associated with the instability of the realization of the buckling process because of the high density of the critical load spectrum.

Experimental Setup and Bar Specimens. Figure 1 shows the specimen loading scheme. The bars 1 were polished steel strips of differing thickness h and width b. Either foam rubber or vacuum rubber with stiffnesses c = 0.47 and 11.5 kg/cm^2, respectively, was used as the elastic base 2, which was bonded to the steel strips. For the measurement of the deformation, the specimen was attached to a toolmaker's microscope on the rigid beam 3, which was bonded to the elastic base. The load was applied to the specimen symmetrically relative to its ends and was measured by the dynamometer 4 with sensitivity $2.7 \cdot 10^{-3}$ kg. The transverse displacements of the flexible bar were measured with accuracy to 10^{-3} mm along its entire length for each fixed load.

The results of the experiments conducted for the nine specimens are presented in the Table, where L is the bar length, N is the experimentally obtained number of halfwaves of the deflected bar, P_0 is the minimal load at which deflection of the bar centerline from a straight line was noted, P_h is the load at which the transverse displacement of the bar centerline reached the thickness h of the elastic bar, P_m is the maximal load applied to the specimen, a is the maximal transverse displacement of the bar centerline, corresponding to the maximal load P_m, n is the theoretically obtained number of halfwaves of the sinusoid, corresponding to the classical linear theory, P_i is the classical critical buckling load of the bar on the elastic base,

Novosibirsk. Translated from Prikladnaya Mekhanika i Tekhnicheskaya Fizika, No. 5, pp. 106-112, September-October, 1994. Original article submitted August 16, 1993; revision submitted January 15, 1994.

0021-8944/94/3505-0739$12.50

TABLE 1

Specimen number	L, mm	Experiment						Theory			
		N	bar behavior	P_0	P_h	P_m	a, mm	n	P_i, kg	bar behavior	
				kg							
1	30	3	V	1,2	2,5	4,6	1,15	3	$P_2 = 3,35$ $P_3 = 2,81$ $P_4 = 3,58$	V V Λ	V V Λ
2	54	6	Λ	1,5	2,6	3,1	0,26	5	$P_4 = 3,03$ $P_5 = 2,77$ $P_6 = 2,97$	V V V	V V Λ
3	74	7	Λ		2,6	4,6	0,9	7	$P_6 = 2,85$ $P_7 = 2,77$ $P_8 = 2,92$	V V V	V V V
4	52	3	V	0,5	1,1	1,5	1,8	2	$P_1 = 1,35$ $P_2 = 0,56$ $P_3 = 0,69$	V V Λ	V V Λ
		4	Λ	0,5	1,5	2,1	0,8		$P_4 = 1,05$	Λ	Λ
5	62	4	Λ	0,56	1,2	1,5	0,9	3	$P_2 = 0,63$ $P_3 = 0,59$ $P_4 = 0,80$	V V Λ	V V Λ
		5	Λ	0,56	1,3	1,5	0,5		$P_5 = 1,14$	Λ	Λ
6	80	5	0	0,4	1,0	1,4	2,1	3	$P_3 = 0,57$ $P_4 = 0,60$ $P_5 = 0,76$	V V Λ	V Λ Λ
7	100	6	Λ	0,5	1,3	1,7	0,5	4	$P_3 = 0,68$ $P_4 = 0,56$ $P_5 = 0,60$ $P_6 = 0,72$	V V V Λ	V V Λ Λ
8	125	7	Λ		0,6	1,3	1,6	5	$P_4 = 0,63$ $P_5 = 0,56$ $P_6 = 0,58$ $P_7 = 0,67$	V V V Λ	V V V Λ
9	120	3	Λ	1,2	4,2	4,5	1,2	3	$P_2 = 2,44$ $P_3 = 2,38$ $P_4 = 3,31$	V V Λ	V Λ Λ
		4	Λ	1,2	3,8	4,2	0,8		$P_5 = 4,77$	Λ	Λ

when i halfwaves are realized. The fourth column and the last two columns of the Table indicate the experimentally recorded and theoretically predicted [7] stable Λ, unstable V, or indifferent 0 postbuckling behavior of the bar. In the last two columns of the Table there are noted the stable and unstable behavior with respect to the i-th mode of the bar-plus-elastic-base system, where the calculations were made using the classical (next-to-last column) and nonclassical (last column) models [7]. The dual rows for the 4-th, 5-th, and 9-th specimens reflect the results of experiments on the same specimens with repetitive loading.

The disturbances that were uncontrollable during loading of the specimens led to differing realizations of the buckling of the bar-plus-elastic-base system. In specimens 1, 2, 3 the elastic base stiffness was c = 11.5 kg/cm^2, in the other specimens c = 0.47 kg/cm^2. For specimen 9 we used a steel strip of thickness h = 0.27 mm and width b = 8 mm, for the other specimens h = 0.1 mm and b = 10 mm. In the calculations the value of the elastic modulus of the steel was taken to be E = $2.0 \cdot 10^6$ kg/cm^2. The stiffness of the elastic base was measured on rubber specimens in which the rubber was not bonded to the steel strips.

Comparison with Theory. The critical loads and the initial periodic buckling modes of an ideal bar of length L that is axially compressed by the load P can be determined from the linearized differential equation of equilibrium of the bar [8]

$$EIy_{xxxx} + Py_{xx} + cy = 0.$$

Here EI is the bending stiffness; c is the bedding coefficient; the function y(x), $0 \le x \le l$ (l is the distance between the ends of the deflected bar, Fig. 2) describes the deformed position of the bar [7] and must satisfy the geometric end conditions of hinged support:

$$y(0) = y(l) = y_{xx}(0) = y_{xx}(l) = 0.$$

For the calculation of the critical load we use the expression [8, 9]

$$P_n = P_*(n^2 + r/n^2), \tag{1}$$

where $P_* = EI(\pi/L)^2$ is the Euler critical load for the bar without the elastic base and $r = c(L/\pi)^4$ is the dimensionless stiffness of the elastic base. The theoretical number n (see the Table) of halfwaves of the sinusoid (corresponding to the initial buckling of the bar) is determined from the condition

$$(n-1)^2n^2 \le r \le n^2(n+1)^2.$$

Table 1 presents the critical loads P_i, calculated using (1), for the modes with number of halfwaves close to n. The theoretical number of halfwaves n is normally less than the experimental number N; for example, for the specimens 4, 5, 6, 7, 8 the difference is two halfwaves. It is clear that an important role is played by the high density of the values of the critical loads (see Table 1) and the multiplicity of the smallest characteristic value (specimens 6, 7, 8, for which the first two critical loads nearly coincide). Thus, for the specimen 8 the fourth in magnitude critical load differs from the first critical load by less than 20 %. The influence of the end effect and the presence of the inevitable initial irregularities also are significant. For example, if for the specimen 5 we take h = 0.107 mm in place of 0.1 mm or for the specimen 9 we take L = 118 mm in place of 120 mm, then for the number of halfwaves in both cases n = 2 in place of n = 3.

We see from Table 1 that for the specimens 1, 2, 3 with base stiffness c = 11.5 kg/cm^2 the theoretical critical load is closer to P_h, while for the specimens 4, 5, 6, 7 (c = 0.47 kg/cm^2) this load is closer to P_0, i.e., closer to the minimal load at which deviation of the bar from a straight line was observed. Thus, we can say that the theoretical n and the experimental N numbers of halfwaves are very sensitive to small changes of the coefficients of the equation and to disturbances in the course of the experiment. From this we can conclude that the influence of the initial irregularities is probably greater on the specimens with the stiffer rubber. We further note that the very simple model of the elastic base, when only a single bedding coefficient is specified, does not describe the shearing that arises in the elastic base [6]. Therefore it is not possible to explain the difference between n and N solely by the influence of the initial irregularities. This may be associated with the nonlinearity of the properties of the elastic base at comparatively large deflections.

For the description of the initial postbuckling behavior of the bar we take the expression for the overall potential energy of the system in the form [4, 10]

$$U = \frac{1}{2}EI\int_0^L w_{ss}^2(1 + w_s^2)ds - P\int_0^L \left(\frac{1}{2}w_s^2 + \frac{1}{8}w_s^4\right)ds + \frac{1}{2}c\int_0^L w^2 ds \tag{2}$$

and write the Euler equation of this functional

$$EIw_{ssss} + EI(w_{ss}^2 + 4w_sw_{sss})w_{ss} + P(1 + \frac{1}{2}w_s^2)w_{ss} + cw\left(1 - \frac{1}{2}w_s^2\right) = 0. \tag{3}$$

We obtain by the perturbation method the relation [7]

$$P_n = P_*[n^2 + r/n^2 + \pi^2(n^4 - 3r)(a/L)^2/8\,], \tag{4}$$

where a is approximately equal to the amplitude of the deflection of the bar. Analyzing (4), we see that the postbuckling behavior of the system is stable for $n^4 > 3r$ and unstable for $n^4 < 3r$. Table 1 also presents the stable and unstable behavior of the system with respect to the mode with i halfwaves, which is predicted by the formula (4) (see also Figs. 4 and 5 in [7]). A schematic graph of the behavior of the systems is shown in Fig. 3, where the Curves 1 and 2, 3 and 4, 5 and 6 correspond to the stable, indifferent, and unstable postbuckling behavior; the lines with odd numbers describe the ideal systems, while the lines with the even numbers describe the nonideal systems.

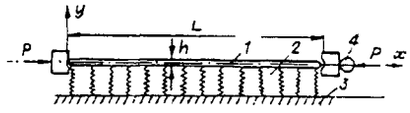

Fig. 1

For the specimen 1 the buckling with 3 halfwaves was found to be unstable in the experiment (see the fourth column of Table 1), in complete agreement with the theory. After reaching the maximal load of 4.62 kg, the symmetry of the specimen 1 broke down and the load decreased to 3.7 kg (Fig. 4); the specimen took the shape shown schematically in Fig. 4, i.e., the periodicity of the buckling mode broke down and local buckling appeared. One of the causes of buckling localization is the density of the critical load spectrum (see, for example, the relation (2.12) in [7]). Another cause are the shear deformations, which can be taken into account in the framework of the approach adopted in [7] with the use of a refined model of the elastic base [6] (see the discussion below of the experimental results).

The mathematical model of the behavior of a bar on an elastic base, in which (2) is taken as the basic relation, has some drawbacks. Thus, the overall potential energy (2) of the bar–base system, when the bar takes the form of a sinusoid with n halfwaves and the amplitude a, has the form [7] (with accuracy to quantities of higher order of smallness)

$$U_n \approx EI(\pi/L)^6 La^4[-n^6 + 3n^2 r]/64.$$

The quantity U_n takes positive values for $r > n^4/3$, although the energy of the unbuckled state is equal to zero ($w \equiv 0$). Thus, in this model the overall potential energy of the buckled state of the system may be greater than the energy of the unbuckled state, and therefore the bar will not buckle. This drawback is not present in the nonclassical model of [7], in which the last term of the formula (2), accounting more precisely for the work of the elastic base, is written in the form

$$c\int_0^L \int_0^w w(1 - w_s^2)^{1/2} dw ds. \tag{5}$$

For the nonclassical model of [7] the potential energy

$$U_n \approx EI(\pi/L)^6 La^4[-n^6 - 4n^2 r]/64,$$

i.e., the energy of the buckled state for any n and r is always less than the energy of the unbuckled state and, consequently, the rectilinear bar equilibrium mode is unstable. For the load-deflection relation in this model we have

$$P_n = P_*[n^2 + r/n^2 + \pi^2(n^4 - 2r)(a/L)^2/8]. \tag{6}$$

Since the Euler equation for the refined functional differs from equation (3) only in the last term, these two theories are easily compared [7]. The system stability characteristic, calculated on the basis of formula (6), is presented in the last column of Table 1. For the specimens 2 and 9 we obtain in this model stable postbuckling behavior with respect to the modes with 6 and 3, respectively, halfwaves of the sinusoid, in full agreement with experiment. The difference between the experimental results for the specimen 6 and the theoretical predictions can be explained by the technical limitations in the tests that were due to the loading device. On the whole, we can conclude that the model in which the work of the elastic base is taken into account by the expression (5) agrees better with the experimental results.

In Figs. 4-6 the solid lines represent the semisums of the amplitudes of the extreme halfwaves, and the dashed lines represent the semisum of the amplitudes of the neighboring halfwaves of the bar, respectively, for the specimens 1 and 4 (the upper row of Table 1 for this specimen) and the specimen 6; on the dashed curves of Figs. 4 and 5 the arrows indicate the reverse motions, when unloading of the neighboring segments of the bar took place because of the unstable behavior of the bar-base system; the buckling modes are shown at the bottom in each of the Figs. 4-6. As a result of the selection of the stiffness of the measuring device 4 (see Fig. 1), it was possible in the experiments to record the unstable postbuckling behavior (the solid lines in Figs. 4 and 5) and the indifferent postbuckling behavior (solid line in Fig. 6).

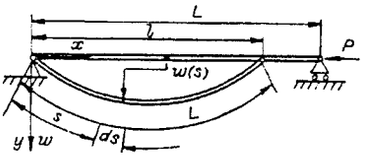

Fig. 2

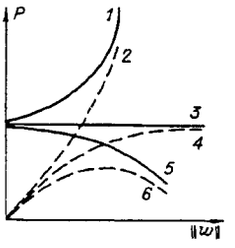

Fig. 3

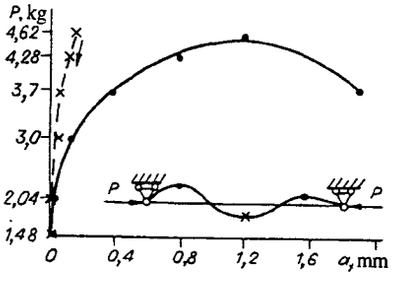

Fig. 4

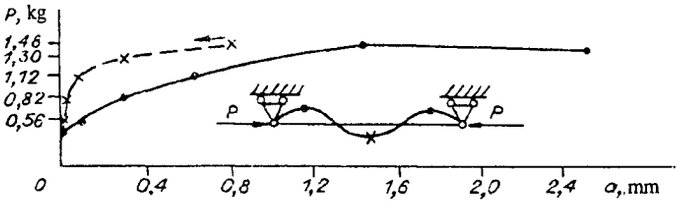

Fig. 5

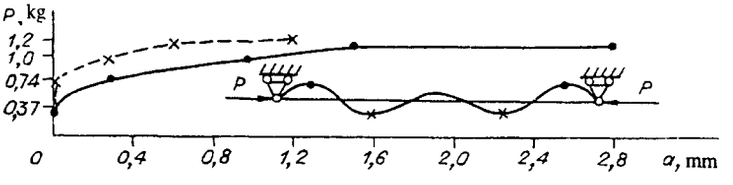

Fig. 6

The experimental results confirmed the disruption of the initial periodic buckling mode of the bar with increase of the load [1, 2] and demonstrated localization of the buckling near the ends of the bar, the latter showing up particularly clearly for buckling with a large number of halfwaves (for example, seven halfwaves for the specimens 3 and 8). Unfortunately, this effect is not captured by the theory, since in the elastic base models used in [7] the shearing deformations were not considered; as a consequence of refinement of the model of the elastic base there appear variable compressive stresses in the bar, which leads to localization of the buckling process in the vicinity of the action of the maximal compressive stresses. It is probably fundamentally possible to evaluate experimentally the magnitude of the averaged compressive stresses acting on each halfwave length by making special additional measurements. We note that the recorded growth of the amplitudes of the neighboring halfwaves (dashed curves in Figs. 4-6) seem to predict stable postbuckling behavior of the system; this is as it should be, since the dashed curves correspond to the small initial segments of the solid curves of each of the figures for moderate deflections.

In the case of repeated loadings of all the specimens, there was obtained on some of the specimens good reproducibility of the experimental results with the uncontrollable disturbances, while on the other specimens under the same conditions (see the experimental results for the specimens 4, 5, 9 in the Table) there was a reconfiguring of the buckling modes, associated with the instability of the realization of the buckling process because of the high density of the spectrum of the critical loads (the values of P_i in the table). The longitudinal loads with finite deflections of the system also vary significantly, depending on the realization of the particular buckling mode. It is advisable not only to monitor the disturbances that arise in the process of the experiment but also to use a more exact model, describing the work of the elastic base, to exclude the theoretical inaccuracies of the determination of the critical loads.

Thus, we were able to demonstrate experimentally the unstable postbuckling behavior of the deformable system consisting of a bar plus an elastic base with finite deflections. For a more complete description of the experimental results relating to the localization of the buckling process it is necessary to formulate a refined mathematical model of the subject system, in which relations of the Vlasov–Leont'ev type [6] are used to describe the work of the elastic base.

REFERENCES

1. V. Tvergaard and A. Needleman, "On the development of localized patterns," in: Collapse: the Buckling of Structures in Theory and Practice [Russian translation], J. M. T. Thompson and G. W. Hunt (eds.), Nauka, Moscow (1991).
2. M. Potier-Ferry, "Amplitude modulation, phase modulation, and localization of buckling patterns," Ibid.
3. A. N. Guz', Mechanics of the Failure of Composite Materials in Compression [in Russian], Nauk. Dumka, Kiev (1990).
4. S. P. Timoshenko, Stability of Elastic Systems [Russian translation], OGIZ, Moscow–Leningrad (1946).
5. F. S. Yasinskii, Selected Works on the Stability of Compressed Bars [in Russian], GITTL, Moscow–Leningrad (1952).
6. V. Z. Vlasov and N. N. Leont'ev, Beams, Plates, and Shells on an Elastic Foundation [in Russian], Fizmatgiz, Moscow (1960).
7. N. S. Astapov and V. M. Kornev, "Postbuckling behavior of an ideal bar on an elastic foundation," PMTF, No. 2 (1994).
8. A. S. Vol'mir, Stability of Deformable Systems [in Russian], Nauka, Moscow (1967).
9. N. A. Alfutov, Fundamentals of Elastic System Stability Calculation [in Russian], Mashinostroenie, Moscow (1991).
10. J. M. T. Thompson, Instabilities and Catastrophes in Science and Engineering [Russian translation], Mir, Moscow (1985).